# Solid State Lasers: Materials and Applications

Sino-American Topical Meeting
and Tabletop Exhibit

**Technical Digest**

**July 8–11, 1997**
**Nankai University**
**Tianjin, PRC**

COS
Chinese Optical Society

OSA
Optical Society of America

*Managed and sponsored by:*
**OSA—Optical Society of America**
**COS—Chinese Optical Society**

# Crystal growth, structural and full optical characterizations of 3-Methyl-4-methoxy-4'-nitrostilben (MMONS)

**Hyung-Ki Hong and Choon Sup Yoon**

*(Dept. of Physics, KAIST, Daeduck Science Town, Taejon, 305-701, Korea.*

*Tel : +82-42-869-2532)*

**Tiejun Xia and E. W. Van Stryland**

*(CREOL, University of Central Florida, Orlando, Florida 32816-2700, USA*

*Tel : +1-407-823-6814)*

Organic crystals with large second-order nonlinear optical (NLO) susceptibilities are of great interest because of their potential use of optical parametric generation.(1) In recent years second-order cascading effects in organic crystals draw much attention not only in the context of basic understandings of the nonlinear optical processes but also potential applications in optoelectronics.

3-Methyl-4-methoxy-4'-nitrostilben (MMONS) is a very promising organic NLO material and the preliminary studies on nonlinear optical properties were reported by Bierlein et al.(2) Single crystals of a large size ($40\times30\times30mm^3$) and of high perfection was successfully grown by solution growth method using methyl ethyl ketone as a solvent. A good quality seed was introduced into the saturated solution and the temperature of the solution was lowered to establish supersaturation at the rate of 0.3°C/day. The crystal structure of MMONS was determined by single crystal X-ray diffraction using a Enraf-Nonius CAD-4 diffractometer. MMONS crystals belong to space group Aba2 ( point group mm2, Z=8 ) with lattice parameters a = 15.750 Å, b = 13.470 Å, c = 13.356 Å.(3) Fig. 1 shows the molecular structure of MMONS. The MMONS molecule has a permanent dipole moment along the charge transfer axis. When it is crystallized, the molecular dipole moments are summed up to cancel out each other in the crystallographic a- and b-axes, but a net dipole mement remains along the polar c-axis, which manifests strong polar nature of the crystal. This polar nature not only strongly affects the crystal growth process but also overall linear and nonlinear optical properties. Defects in a crystal can affect not only mechanical properties but also optical properties as well. It was therefore necessary to make a defect characterization by using white beam synchrotron X-ray topography. The X-ray topographs of 002 reflection reveal the details of growth sector boundary, strain fields and dislocations of mixed type. The dislocation density was estimated to be an order of $10^2/cm^2$. Laser damage threshold was measured on the (100) plane by using the pulsed Nd:YAG laser. The damage threshold was 56 $MW/cm^2$ for 8 ns pulses, while the threshold goes up as high as 17 $GW/cm^2$ for the beam of 30 ps pulse width. From the linear

refractive index data of MMONS, the phase matching angles for type I and type II and the corresponding walk-off angles were calculated. The type II phase matching at ($\theta$, $\phi$) = (73.13°, 0°) gives the largest value of the effective second-order nonlinear coefficint, $d_{eff}$ = 59 pm/V. The full coefficients of the second-order nonlinear susceptibility tensor were measured by using the Maker fringe technique [Fig.2] and $d_{31}$ component was determined for the first time. However the measured value of $d_{33}$ ( 80 pm/V) is smaller than that of Bierlein's and this is probably due to the fact that Bierlein et al used the wrong $d_{33}$ value of KTP as a reference. Utilizing the birefringence of the crystal, the second harmonic generations of type I and type II collinear phase matchings were exploited. Maximum conversion efficiencies of 2.5 % for type I and 13 % for type II were obtained at 1064 nm.

Nonlinear refractive indices and absorption coefficients were measured by using Z-scan technique at 532 nm and 1064 nm for the polarizations parallel to the crystallographic b- and c-axes[Fig.3]. Linear absorption coefficients were also derived from the Z-scan geometry. The measured values of nonlinear refractive index $n_2$, two-photon absorption coefficient $\beta$ and linear absorption coefficient $\alpha_0$ are summarized in Table 1, where $n = n_0 + n_2|E|^2/2$ and $\alpha = \alpha_0 + \beta I$. The linear absorption coefficients for the polar c-direction are twice as large as those for the nonpolar b-direction both at the fundamental and harmonic wavelengths, which is the consequence of highly anisotropic distribution of $\pi$-electrons along the polar c-axis. The much larger values of the nonlinear refractive index $n_2$ and the two-photon absorption coefficient $\beta$ in the polar c-direction than those in the nonpolar b-direction clearly indicate that the nonlinear effect occurs predominantly along the molecular charge transfer direciton. Open aperture Z-scan data shows that the multiphoton rather than two-photon processes are involved at 1064 nm. Assuming that three-photon absorption dominate in the nonlinear absorption processes at 1064 nm, the three-photon absorption coefficient for the c-polarization was estimated to be $\eta$ = - 0.62 $cm^3/GW^2$.

Table 1. Complex nonlinear refractive indices and linear absorption coefficients.

| | $\lambda$ = 532 nm | | $\lambda$ = 1064 nm | |
|---|---|---|---|---|
| | b-polarization | c-polarization | b-polarization | c-polarization |
| $\alpha_0$ ($cm^{-1}$) | 2.24 | 4.95 | 0.54 | 1.01 |
| $\beta$ (cm/GW) | 7.37 | 34.2 | 0 | 0 |
| $n_2$($10^{-12}$ esu) | 4.9 | 71.8 | 1.9 | 5.6 |

**References**


1. S.X.Dou and D.Josse and J.Zyss, J.Opt.Soc.Am.B **10**, 1708(1993).
2. J.D.Bierlein, L.K.Cheng, Y.Wang and W.Tam, Appl.Phys.Lett **56**, 423(1990).
3. Il-Hwan Suh, Sung-Su Lim, Jin-Ho Lee, Bo-Young Ryu, Moon-Jib Kim, Choon Sup Yoon, Hyung-Ki Hong and Kwang Sup Lee, Acta Cryst. **C 50**, 1768(1994).

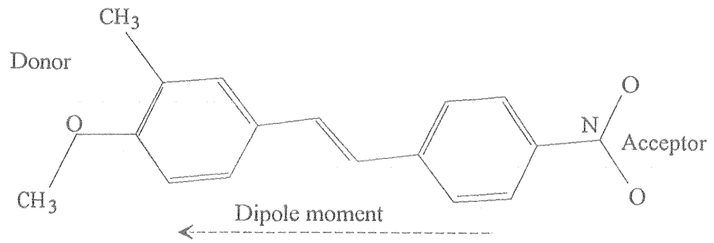


Fig.1 Molecular structure of MMONS.

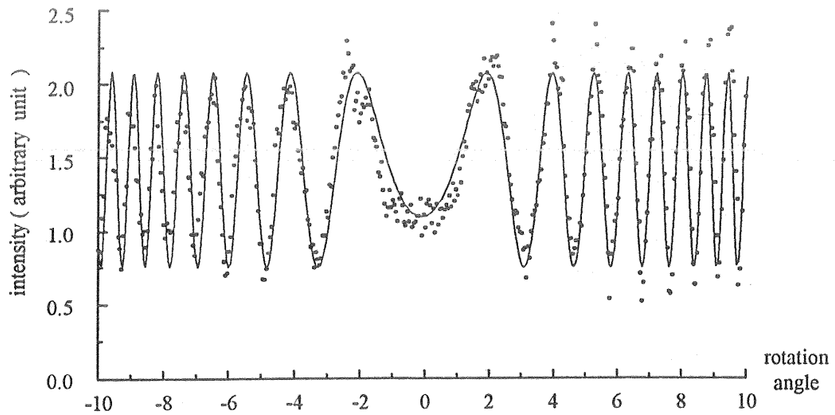


Fig.2 Maker fringe of a-cut MMONS sample. The closed circles represent measured values and the solid curve calculated one.

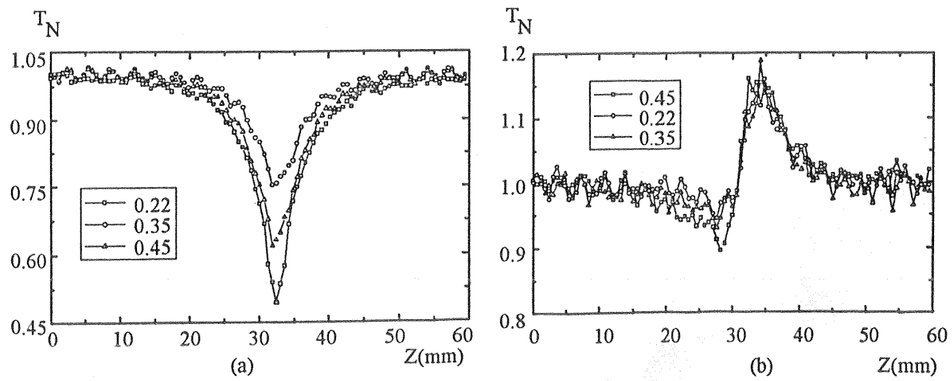


Fig.3 Z-scan transmission for the c-polarization at 532 nm for (a) open aperture and (b) closed aperture.